



## COMPUTATIONAL FLUID DYNAMICS MODELING OF FLOW CHARACTERISTICS OVER V-NOTCH SIDE WEIRS

T. A. Ewemoje\* and P. D. Salau

Department of Agricultural and Environmental Engineering, Faculty of Technology, University of Ibadan, Ibadan, Nigeria.

\*Corresponding Author Email: tayo\_ewemoje@yahoo.co.uk

### ABSTRACT

Side weirs are one of the most important and applicable hydraulic structures for water control and diversion systems that require careful review and accurate design due to their critical importance. In this study, flow characteristic over a V-notch side weir in a rectangular channel was carried out experimentally. Simulation was also carried out using Computational Fluid Dynamic (CFD) to describe the discharge coefficient ( $C_d$ ). A relationship between discharge coefficient ( $C_d$ ), Froude number ( $Fr$ ) and Reynolds number ( $Re$ ) were established with dimensional analysis and their linear and multiple regression models were fitted using Statistical Package for the Social Sciences (SPSS) for correlation test at 95% confidence. Simulation of flow was carried out using COMSOL Multiphysics (5.0) software. The discharge coefficient ( $C_d$ ) for no sill height V-notch side weirs with no downstream weir ranged from 0.13 to 0.28. The  $C_d$  for no sill height V-notch side weirs with rectangular downstream weir ranged from 0.70 to 0.93 and that for 5cm sill height V-notch side weir with rectangular downstream weir ranged from 0.63 to 0.75. The relationship established with dimensional analysis is  $C_d = f\left(\frac{H}{p}, Fr, \frac{H}{B}, Re, \theta, S_0\right)$ , indicating that the discharge coefficient is a function of the other parameters. Comparison of experimental and simulated results gave a good similarity with no sill height V-notch side weir, having 5cm rectangular downstream weir with Root Mean Square Error (RMSE) of 25% for  $60^\circ$  and 1% for  $90^\circ$  and  $120^\circ$ . However, there is a wide discrepancy for 5cm sill height V-notch side weir having 5cm rectangular downstream weir with RMSE that ranged from 30 to 57%.

**Keywords:** Side weir, Sill height, Discharge coefficient, Dimensional analysis, CFD.

### INTRODUCTION

A weir is an obstruction in an open channel that water must flow over usually through an opening, or notch of regular form, and is used as an indirect method for obtaining the discharge based on the height of water over the weir crest known as head and the weir geometry (Abd el-hady rady, 2011). Side weirs are overflow weirs set into the side of a channel and is used for water level control in canal systems, diverting excess water into relief channels during floods and as head regulators of distribution (Ogedengbe and Ewemoje, 2001). These structures help the flood flow deviate from the main stream to non-hazard zone without any significant side effects compared to other mitigations such as dams or retention ponds (Nezami *et al.*, 2015). One of the functions of side weir in a channel is to divert water into agricultural field for the purpose of irrigation, hence, it is imperative to determine accurately the quantity of water discharge through it to avoid flooding of the field (Eghbalzadeh *et al.*, 2015). Like all typical weirs, side weirs can be broad crested or sharp crested with various geometrical shapes such as trapezoidal, triangular, rectangular, etc. (Parsaie and Haqjab, 2013). According to Shahaboddin *et al.* (2016), flows through side weirs are typical examples of spatially varied flow (SVF) with decreasing discharge. Spatially varying flow condition occurs in an open channel when the flow depth changes gradually due to the changes in the discharge along the length of the channel which is as a result of outflow or inflow of water from the channel boundaries (Mangarulkar, 2010). However, flood can be controlled by allowing large volumes of water to be detained and released slowly at an acceptable rate by diverting some of the volume of water and this discharge rate is controlled by structures

such as side weirs (Spencer, 2013). Thus, Abdullahi, (2014) stated that in irrigation there is the need for water to be measured accurately.

Computational fluid dynamics (CFD) can be defined as the science of predicting fluid flow, heat and mass transfer, chemical reactions and related phenomena by solving the mathematical equations which govern these processes using a numerical process (Bakker, 2006). The CFD provides a qualitative and quantitative method of predicting fluid flows by means of mathematical modeling (partial differential equations), numerical methods (discretization and solution techniques) and software tools (Kuzmin, 2016). The adopted governing equation is the Reynolds Averaged Navier Stokes (RANS) equation (Mohammadighavam, 2017). Compared with experimental testing, computer modeling offers possible savings; it removes the necessity for a sophisticated physical model and presents the possibility of less iteration to the final design with less expensive prototypes to produce (Douglas, *et al.*, 2005). There is dearth of information on comparative study between different angles of V-notch side weir considering sill height, downstream height and three different angles ( $60^\circ$ ,  $90^\circ$  and  $120^\circ$ ) using CFD. Hence, it is unclear the optimum V-notch side weir angle to be used in water diversion. Therefore, the objectives of this work are to investigate flow characteristics over a V-notch side weir, determine the weir discharge coefficient ( $C_d$ ) for different angles of V-notch side weirs, carry out simulation of flow over a V-notch side weir using COMSOL Multiphysics and compare the simulation results with the experimental observations. According to Rajput, (2013) the theoretical

and actual discharge over a V-notch weir is given as Equations (1) and (2).

$$Q_{the} = \frac{8}{15} \sqrt{2g} \tan \frac{\theta}{2} (H)^{\frac{5}{2}} \quad (1)$$

$$Q_{act} = \frac{V}{t} \quad (2)$$

Where: Q is the theoretical discharge over the V-notch in m<sup>3</sup>/s, g is acceleration due to gravity in m/s<sup>2</sup>, θ is the angle of the V-notch and H is the flow depth above the side weir in m, V is the volume of water collected in m<sup>3</sup> and t is time in seconds.

**MATERIALS AND METHODS**

Experimental work was carried out at the Soil and Water Conservation Engineering Laboratory of the Department of Agricultural and Environmental Engineering, University of Ibadan in June 2017. Experimental flow channels were constructed using Perspex glass plate of 3 mm thickness. The channels are hydraulically smooth rectangular open channel; 1100 mm length, 100 mm width and 150 mm height, having a V-notch side weir on one side of the wall. The side weir center was positioned at a distance of 400 mm

from the channel inlet after the transition section which is 100 mm from the inlet. Nine open channels were constructed having three different degrees of V-notch side weir of 60°, 90° and 120°. The first three were open channels with V-notch side weirs of no sill height, having a free flow downstream, followed by three open channels with V-notch side weirs of no sill height, having a 5 cm sill height rectangular weir downstream and lastly, three open channels with 5 cm sill height V-notch side weirs having a 5 cm sill height rectangular weir downstream (Plates 1 and 2). The flow enters into all the experimental channels from a constant head tank which water is delivered into from a main tank during experimentation. All channels were placed on a leveled wooden work bench when carrying out the experiment. The water passes through a transition section of 100 mm filled with small grains of gravels and glass mesh to reduce turbulence in the flow. The actual discharge (Q<sub>act</sub>) over the side weir was measured using volumetric method with the use of calibrated bucket while the upstream height of water over the crest of the weir (H) was measured with a point gage to the nearest millimeter (Plate 3).



Plate 1: V-notch side weir of no sill height

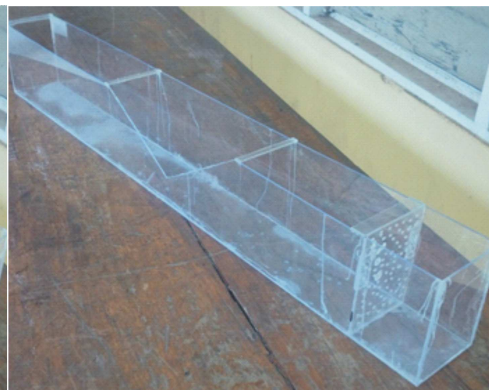


Plate 2: 5 cm sill height V-notch side weirs



Plate 3: Experimental setup behind soil and water laboratory

### Discharge (Q)

The actual discharge ( $Q_{act}$ ) of main channel and the side weir was measured using gravimetric method with the use of calibrated buckets and converted to  $m^3/s$ . The inlet discharge was computed by applying the continuity equation.

Where:

$$Q_{in} = Q_{SW} + Q_{DS} \quad (3)$$

$Q_{in}$  is discharge entry into the channel;

$Q_{SW}$  is discharge at the V-notch side weir, and

$Q_{DS}$  is discharge at the downstream session of the channel.

### Discharge coefficient ( $C_d$ )

The discharge coefficient for the V-notch side weir was computed with the use of Equations (1) and (2). Equation (1) represents the measured discharge through the V-notch side weir. The discharge coefficient ( $C_d$ ) was computed using Equation (4).

$$C_d = \frac{Q_{act}}{Q_{theo}} \quad (4)$$

### Froude's Number ( $Fr$ )

The upstream Froude's number which defines the regime of flow before the side weir is calculated using the Equation (5).

$$Fr = \frac{v}{\sqrt{gD}} \quad (5)$$

Where:  $v$  is the velocity upstream,

$g$  is the acceleration due to gravity,

$D$  is the hydraulic depth.

### Reynolds number ( $Re$ )

The Reynolds number which determines if a flow is laminar or turbulent was calculated using Equation (6).

$$Re = \frac{\rho v D}{\mu} \quad (6)$$

Where:

$\rho$  is the density of water;

$v$  is the velocity of flow upstream before side weir;

$D$  is the hydraulic depth;

$\mu$  is the dynamic viscosity of water at room temperature.

Equations (3)-(5) were also used in calculating discharge coefficient, Reynolds number and Froude number for the simulated results.

### COMSOL Multiphysics Procedure

The flow over the V-notch weirs was modeled with COMSOL Multiphysics (5.0) with 3D Space dimension. Since the flow was turbulent, Turbulent Flow, k- $\epsilon$  (spf) model was used as the physics (The physics interface used for modelling the flow in the experimental channels is incompressible flows at low Mach number (typically less than 0.3) while the equations solved by the Turbulent Flow, k- $\epsilon$  interface are the Navier-Stokes equations for conservation of momentum and the continuity equation for conservation of mass), the study type was assumed as stationary (steady state). A solid block was created having same dimension of width and length as the experimental channel but the height was the height of upstream water

head measured during experiment. V-notch side weir was created using polygon line at the same point as it was in the experimental channel. The downstream weir was created by a solid rectangle of same dimension as the experimental channel attached to the end of the solid block. The boundary condition for the open boundary is that there is no shear stress base on the assumption that the pressure gradient at the atmospheric interface is negligible. The boundary condition for the inlet is the inlet velocity measured from the experiment. The wall boundary condition is slip, which prescribe a no penetration condition, that is no viscous effects at the wall (the main effect of the wall is to prevent fluid from leaving the domain). The outlet boundary was defined as the pressure outlet used to specify constant pressure at the boundary. A coarser mesh (Figure 1) was use for the meshing, so as to reduce computational time.

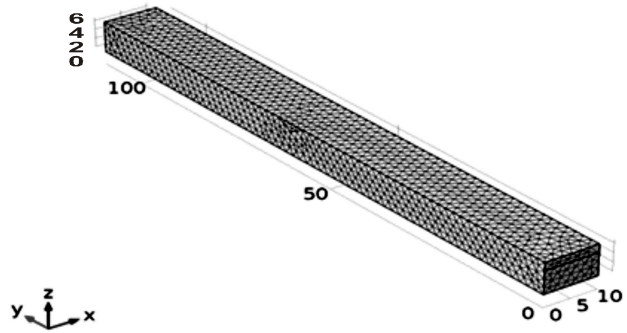


Figure1: Coarser mesh in COMSOL multiphysics

### Dimensional Analysis

The discharge ( $Q$ ) through a V-notch side weir was assumed to be dependent on the head of water above the crest of the V-notch ( $H$ ), mean velocity upstream before side weir ( $V$ ), sill height from the base of the channel to the crest of the weir ( $P$ ), gravitational acceleration ( $g$ ), the channel width ( $B$ ), the viscosity of the fluid ( $\nu$ ), the V-notch angle ( $\theta$ ) and the channel bed slope ( $S_0$ ) and dimensional analysis was carried out on these variables.

$$Q = f(H, V, P, g, B, \nu, \theta, S_0) \quad (7)$$

Buckingham's  $\pi$  theorem was used and  $H$  and  $V$  were chosen as repeating variables, Equations 8 and 9 show the non-dimensional equation formed and dimensional homogeneity respectively, equating to Equation (10) which shows the relationship between the dependent and independent variables.

$$Q = \sqrt{2gH^{\frac{5}{2}} \phi \left( \frac{P}{H}, \frac{gH}{V^2}, \frac{B}{H}, \frac{\nu}{VH}, \theta, S_0 \right)} \quad (8)$$

$$C_d = f \left( \frac{H}{P}, \frac{V^2}{gH}, \frac{H}{B}, \frac{VH}{\nu}, \theta, S_0 \right) \quad (9)$$

But  $\frac{V}{\sqrt{gD}} = \frac{V^2}{gH} =$  Froude's number ( $Fr$ ) and  $\frac{VL}{\nu} = \frac{VH}{\nu} =$  Reynolds number ( $Re$ )

$$C_d = f \left( \frac{H}{P}, Fr, \frac{H}{B}, Re, \theta, S_0 \right) \quad (10)$$

**Statistical Analysis**

The dimensional analysis has shown that  $C_d$  is a function of other  $F_r, R_e, \frac{H}{P}, \frac{H}{B}, \theta$  and  $S_0$  as shown in Equation (10).

Simple linear regression was used to model the relationship between two variables, a dependent variable denoted as Y ( $C_d$ ) and an independent variable denoted as X ( $\frac{H}{P}, F_r, \frac{H}{B}, R_e, \theta, S_0$ ). The regression line Equation is:

$$y = b_1x + b_0 \tag{11}$$

Where:  $b_1$  is slope and  $b_0$  is the intercept.  
The sample correlation coefficient (r) is;

$$r = \frac{SS_{xy}}{\sqrt{SS_xSS_y}} \tag{12}$$

Coefficient of determination ( $r^2$ ) is a descriptive measure of the strength of the regression relationship, that is a measure of how well the regression line fits the data.

∴ Coefficient of determination ( $r^2$ ) can be calculated directly from Equation (13).

$$r^2 = \frac{SSR}{SST} \tag{13}$$

Where: Total sum of squares (SST) = Sum of squares for error (Residual) (SSE) + Sum of square for regression (SSR) (Model).

With the experimental results, the effect of variables was tested linearly and later altogether to develop a mathematical model. The effect of the upstream Froude number Fr was tested first as it has been suggested as the most influential parameter from literatures.

**RESULTS AND DISCUSSION**

**Discharge over V-Notch Side Weir**

The discharge over the V-notch side weir and downstream section of the channel (measured) and the computed inlet discharge presented in Tables 1-9 (all units in  $m^3/s$ ).

Table 1: Discharge for 60 degree no sill height V-notch side weir with no downstream weir

| Side Weir Discharge ( $Q_{SW}$ ) | Downstream Discharge ( $Q_{DS}$ ) | Inlet Discharge ( $Q_{in}$ ) |
|----------------------------------|-----------------------------------|------------------------------|
| 0.000005843                      | 0.0004733                         | 0.00048                      |
| 0.000006936                      | 0.0005687                         | 0.00058                      |
| 0.000009211                      | 0.0005158                         | 0.00053                      |

Table 2: Discharge for 60 degree no sill height V-notch side weir with 5 cm sill height rectangular downstream weir

| Side Weir Discharge ( $Q_{SW}$ ) | Downstream Discharge ( $Q_{DS}$ ) | Inlet Discharge ( $Q_{in}$ ) |
|----------------------------------|-----------------------------------|------------------------------|
| 0.0004000                        | 0.00008                           | 0.00048                      |
| 0.0003846                        | 0.00003462                        | 0.00042                      |
| 0.0003839                        | 0.00004798                        | 0.00043                      |

Table 3: Discharge for 60 degrees, 5 cm sill height V-notch side weir with 5 cm sill height rectangular downstream weir

| Side Weir Discharge ( $Q_{SW}$ ) | Downstream Discharge ( $Q_{DS}$ ) | Inlet Discharge ( $Q_{in}$ ) |
|----------------------------------|-----------------------------------|------------------------------|
| 0.00002496                       | 0.0004409                         | 0.00047                      |
| 0.00004521                       | 0.0005812                         | 0.00063                      |
| 0.00002501                       | 0.0004145                         | 0.00044                      |

Table 4: Discharge for 90 degree no sill height V-notch side weir with no downstream weir

| Side Weir Discharge ( $Q_{SW}$ ) | Downstream Discharge ( $Q_{DS}$ ) | Inlet Discharge ( $Q_{in}$ ) |
|----------------------------------|-----------------------------------|------------------------------|
| 0.00001233                       | 0.0003904                         | 0.00040                      |
| 0.000009429                      | 0.0004023                         | 0.00041                      |
| 0.00001162                       | 0.0005884                         | 0.00060                      |

Table 5: Discharge for 90 degree no sill height V-notch side weir with 5 cm sill height rectangular downstream weir

| Side Weir Discharge ( $Q_{SW}$ ) | Downstream Discharge ( $Q_{DS}$ ) | Inlet Discharge ( $Q_{in}$ ) |
|----------------------------------|-----------------------------------|------------------------------|
| 0.0004367                        | 0.000                             | 0.00044                      |
| 0.0004364                        | 0.000                             | 0.00044                      |
| 0.0003870                        | 0.000                             | 0.00039                      |

Table 6: Discharge for 90 degrees, 5 cm sill height V-notch side weir with 5 cm sill height rectangular downstream weir

| Side Weir Discharge ( $Q_{SW}$ ) | Downstream Discharge ( $Q_{DS}$ ) | Inlet Discharge ( $Q_{in}$ ) |
|----------------------------------|-----------------------------------|------------------------------|
| 0.00002653                       | 0.0003781                         | 0.00040                      |
| 0.00002898                       | 0.0003929                         | 0.00042                      |
| 0.00004740                       | 0.0005333                         | 0.00058                      |

Table 7: Discharge for 120 degree no sill height V-notch side weir with no downstream weir

| Side Weir Discharge ( $Q_{SW}$ ) | Downstream Discharge ( $Q_{DS}$ ) | Inlet Discharge ( $Q_{in}$ ) |
|----------------------------------|-----------------------------------|------------------------------|
| 0.000008856                      | 0.0003897                         | 0.00040                      |
| 0.000007485                      | 0.0004132                         | 0.00042                      |
| 0.000001019                      | 0.0006078                         | 0.00062                      |

Table 8: Discharge for 120 degree no sill height V-notch side weir with 5 cm sill height rectangular downstream weir

| Side Weir Discharge ( $Q_{SW}$ ) | Downstream Discharge ( $Q_{DS}$ ) | Inlet Discharge ( $Q_{in}$ ) |
|----------------------------------|-----------------------------------|------------------------------|
| 0.0004310                        | 0.000                             | 0.00043                      |
| 0.0004004                        | 0.000                             | 0.00040                      |
| 0.0004874                        | 0.000                             | 0.00049                      |

Table 9: Discharge for 120 degrees, 5 cm sill height V-notch side weir with 5 cm sill height rectangular downstream weir

| Side Weir Discharge ( $Q_{SW}$ ) | Downstream Discharge ( $Q_{DS}$ ) | Inlet Discharge ( $Q_{in}$ ) |
|----------------------------------|-----------------------------------|------------------------------|
| 0.0001015                        | 0.0003044                         | 0.00041                      |
| 0.0001139                        | 0.0003275                         | 0.00044                      |
| 0.0001305                        | 0.0003638                         | 0.00049                      |

From the Tables 1-9, the discharge over a V-notch side weir increased with downstream weir. It was observed that the discharge over the 5cm sill height V-notch side weir, having 5 cm rectangular downstream weir was more than that of no sill height V-notch side weir with no downstream weir. This could have occurred as a result of the back flow caused by the downstream weir. For V-notch side weir with no sill height, having a 5 cm downstream rectangular weir, there was no discharge over the downstream stream except for the 60 degrees V-notch side weir. This setting could be used when designing for the complete diversion of water so as to prevent flooding downstream or a channel for water to go

over the crest of the weir downstream at the extreme case of flooding if a V-notch side weir of angle equal to or greater than 90 degrees with no sill height is adopted in a similar manner as that of the experiment carried out.

#### Flow Characteristics in the Channel

The upstream head (H) of water over the V-notch side weir, the upstream Froude's number (Fr) which indicates the flow regime in the channel and the Reynolds number (Re) which describe the dominant forces in the channel are presented in Tables 10-18.

Table 10: Upstream head, Froude's number and Reynolds number of flow for 60 degrees no sill height V-notch side weir with no downstream weir

| H (m) | Fr   | Re   |
|-------|------|------|
| 0.012 | 1.16 | 4697 |
| 0.013 | 1.24 | 5643 |
| 0.014 | 1.01 | 5147 |

Table 11: Upstream head, Froude's number and Reynolds number of flow for 60 degrees no sill height V-notch side weir with 5 cm sill height rectangular downstream weir

| H (m) | Fr   | Re   |
|-------|------|------|
| 0.04  | 0.19 | 4706 |
| 0.038 | 0.18 | 4110 |
| 0.04  | 0.17 | 4234 |

Table 12: Upstream head, Froude's number and Reynolds number of flow for 60 degrees, 5 cm sill height V-notch side weir with 5 cm sill height rectangular downstream weir

| <b>H (m)</b> | <b>Fr</b> | <b>Re</b> |
|--------------|-----------|-----------|
| 0.015        | 0.81      | 4567      |
| 0.019        | 0.76      | 6141      |
| 0.015        | 0.76      | 4309      |

Table 13: Upstream head, Froude's number and Reynolds number of flow for 90 degrees no sill height V-notch side weir with a downstream weir

| <b>H (m)</b> | <b>Fr</b> | <b>Re</b> |
|--------------|-----------|-----------|
| 0.012        | 0.98      | 3948      |
| 0.013        | 0.89      | 4037      |
| 0.016        | 0.95      | 5883      |

Table 14: Upstream head, Froude's number and Reynolds number of flow for 90 degrees no sill height V-notch side weir with 5 cm sill height rectangular downstream weir

| <b>H (m)</b> | <b>Fr</b> | <b>Re</b> |
|--------------|-----------|-----------|
| 0.037        | 0.20      | 4281      |
| 0.037        | 0.20      | 4278      |
| 0.035        | 0.19      | 3794      |

Table 15: Upstream head, Froude's number and Reynolds number of flow 90 degrees, 5 cm sill height V-notch side weir with 5 cm sill height rectangular downstream weir

| <b>H (m)</b> | <b>Fr</b> | <b>Re</b> |
|--------------|-----------|-----------|
| 0.0125       | 0.92      | 3967      |
| 0.013        | 0.91      | 4136      |
| 0.016        | 0.92      | 5693      |

Table 16: Upstream head, Froude's number and Reynolds number of flow for 120 degrees no sill height V-notch side weir with a downstream weir

| <b>H (m)</b> | <b>Fr</b> | <b>Re</b> |
|--------------|-----------|-----------|
| 0.011        | 1.10      | 3907      |
| 0.012        | 1.02      | 4124      |
| 0.014        | 1.19      | 6059      |

Table 17: Upstream head, Froude's number and Reynolds number of flow for 120 degrees no sill height V-notch side weir with 5 cm sill height rectangular downstream weir

| <b>H (m)</b> | <b>Fr</b> | <b>Re</b> |
|--------------|-----------|-----------|
| 0.029        | 0.28      | 4225      |
| 0.028        | 0.27      | 3925      |
| 0.031        | 0.29      | 4778      |

Table 18: Upstream head, Froude's number and Reynolds number of flow for 120 degrees, 5 cm sill height V-notch side weir with 5 cm sill height rectangular downstream weir

| <b>H (m)</b> | <b>Fr</b> | <b>Re</b> |
|--------------|-----------|-----------|
| 0.016        | 0.64      | 3979.41   |
| 0.017        | 0.64      | 4327.45   |
| 0.018        | 0.65      | 4846.08   |

Table 19: Channels with no sill height V-notch side weir, having no downstream weir

| Angle (degrees) | Discharge coefficient ( $C_d$ ) |
|-----------------|---------------------------------|
| 60              | 0.28                            |
| 90              | 0.23                            |
| 120             | 0.13                            |

Table 20: Channels with no sill height V-notch side weir, having 5 cm sill height rectangular downstream weir

| Angle (degrees) | Discharge coefficient ( $C_d$ ) |
|-----------------|---------------------------------|
| 60              | 0.93                            |
| 90              | 0.70                            |
| 120             | 0.73                            |

Table 21: Channels with 5cm sill height V-notch side weir, having 5 cm sill height rectangular downstream weir

| Angle (degrees) | Discharge coefficient ( $C_d$ ) |
|-----------------|---------------------------------|
| 60              | 0.67                            |
| 90              | 0.63                            |
| 120             | 0.75                            |

From the Tables 10-18, the entire flow regime in the channels is subcritical flow except flows in 60° and 120° no sill height V-notch side weir with no downstream weir. In this channel, the Froude's number is greater than one ( $Fr > 1$ ), showing supercritical flow, which indicates that inertia forces dominate this channel (Table 7). The supercritical flow is caused by shallower depths and higher velocities and the wave disturbance cannot propagate upstream. The channels where the Froude's number is less than one (Tables 1-6, 8 and 9) represent subcritical flow (deeper depths and lower velocities). This is an indication that the normal depth of the flow is above critical depth and gravitational forces dominate. That is, the upstream flow is influenced by the condition of the downstream flow which is as a result of the downstream weir as there is a slight elevation of the water head from the downstream weir backward.

The entire flow in the channels exhibit turbulence, (Reynolds number greater than 1000) for open channel flow. This is the flow character of almost all fluid flowing in natural channels. The experiment exhibits the character of real life flow.

#### Discharge Coefficient ( $C_d$ )

The mean discharge coefficient ( $C_d$ ) for each run of experiment and each angle of V-notch side weir are presented in Tables 19-21.

From the tables 19-21, the V-notch side weirs with no sill height and no downstream weir have the least values of discharge coefficient between 0.10 and 0.28, thus indicating the least efficient for the diversion of water from a channel

as almost all inlet discharge flows downstream. The values for the no sill height V-notch side weir, having downstream weir between 0.73 and 0.93 while the V-notch side weir with 5cm sill height, having a downstream weir between 0.63 and 0.75.

#### Simulation of the Flow Experiment using COMSOL Multiphysics

The result obtained when modeling the flow characteristics (head and velocity) over a V-notch side weir are presented in Figures 1-13. It was observed that there is decrease in velocity and increase in pressure downstream. The same trend is observed in each channel in different magnitude. The velocity decreased downstream after the V-notch side weir as shown in Figures 2,4,6,8,10 and 12. This could be an indication of a varied flow with decreasing discharge (water exiting the channel along the flow path through the weir) and it is in agreement with continuity equation, as the mass entering the channel will equal to the mass leaving the channel. In the pressure profiles (Figures 3,5,7,9, 11 and 13), it was observed that there is pressure increase at the downstream end of the channel, which could be an indication that when designing a channel with weir, the downstream section should be reinforced to withstand higher pressure than the rest of the section, so as to prevent failure of such structures. When a cut 3D line was drawn from the crest of the V-notch to the top of the flow to extract the average velocity of flow through the V-notch side weir, it was observed that the velocity at different height varies. The lowest velocity was at the bottom of the channel in contact with channel wall and the highest was just below the top of the flow.

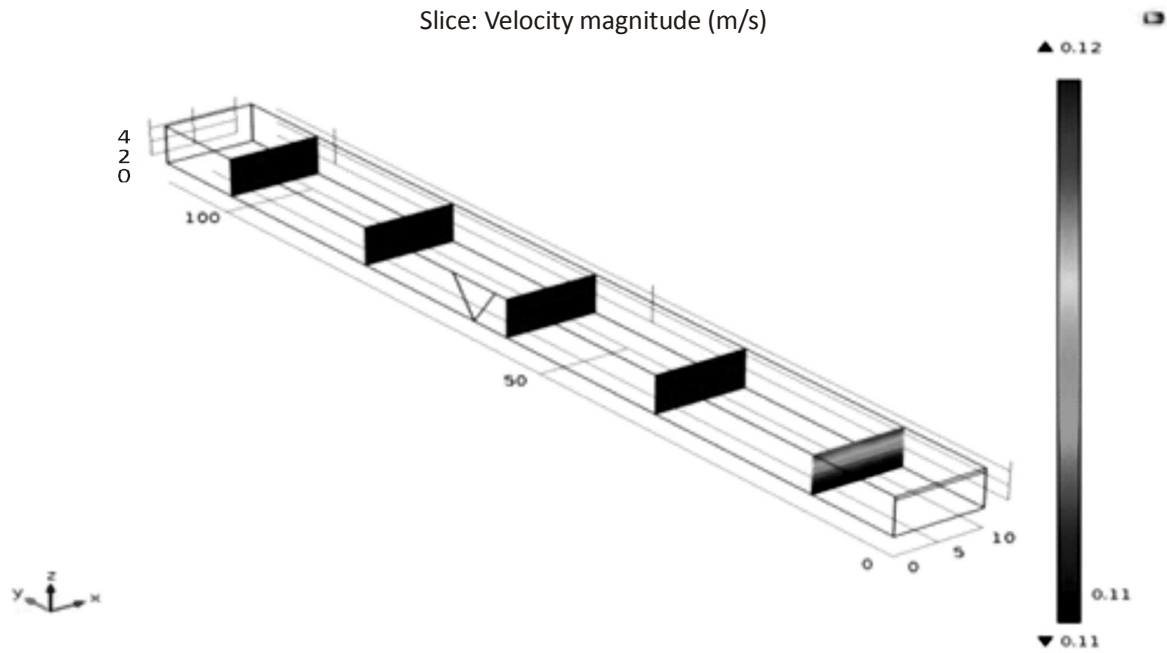


Figure 2: Velocity profile for channel with no sill height 60° V-notch side weir, having downstream weir

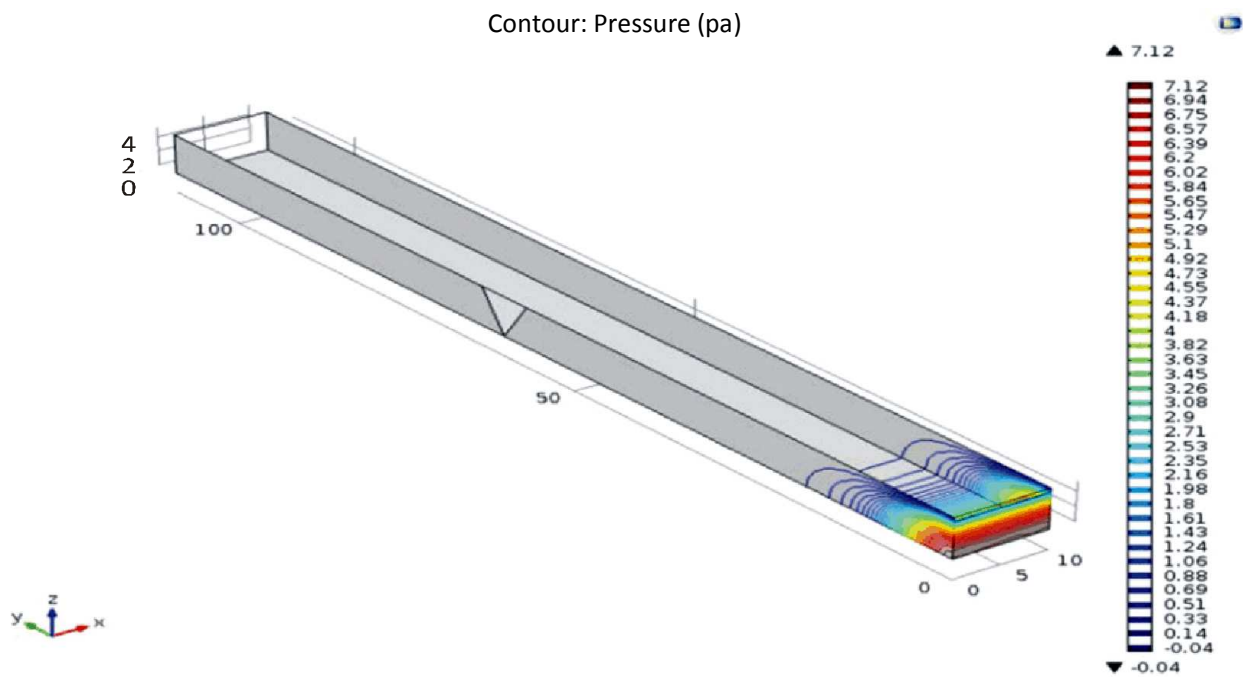


Figure 3: Pressure profile for channel with no sill height 60° V-notch side weir, having downstream weir



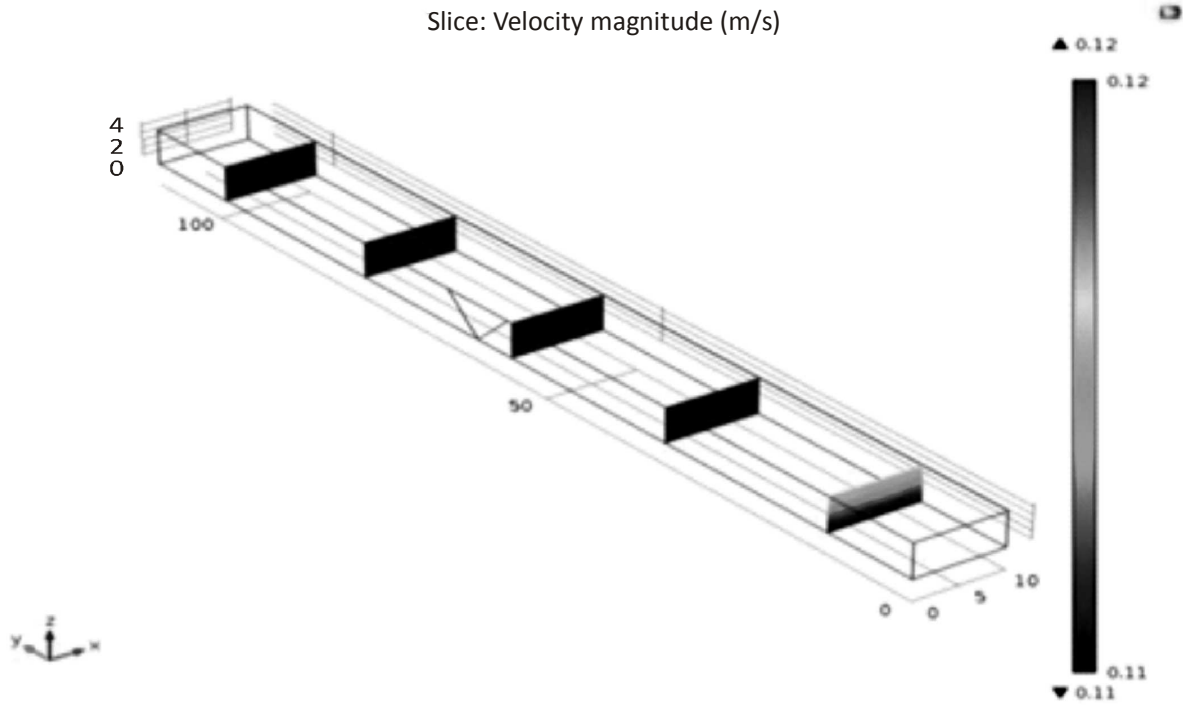


Figure 4: Velocity profile for channel with no sill height 90° V-notch side weir, having downstream weir

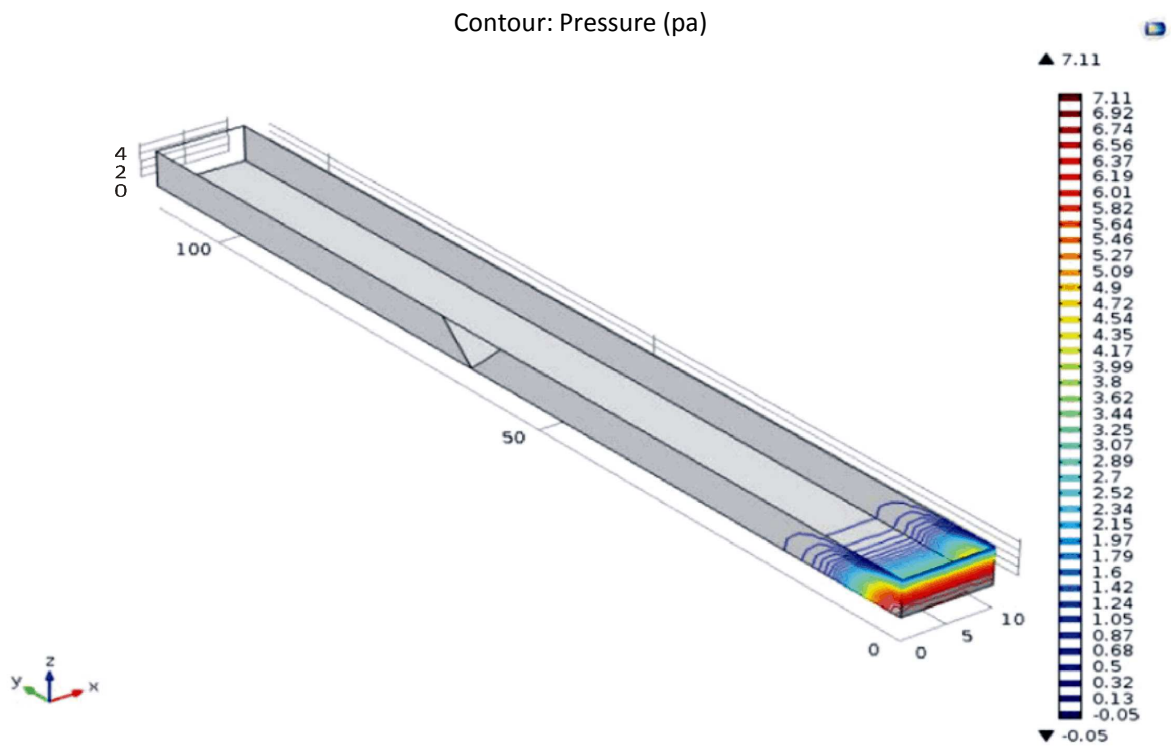


Figure 5: Pressure profile for channel with no sill height 90° V-notch side weir, having downstream weir

Contour: Pressure (pa)

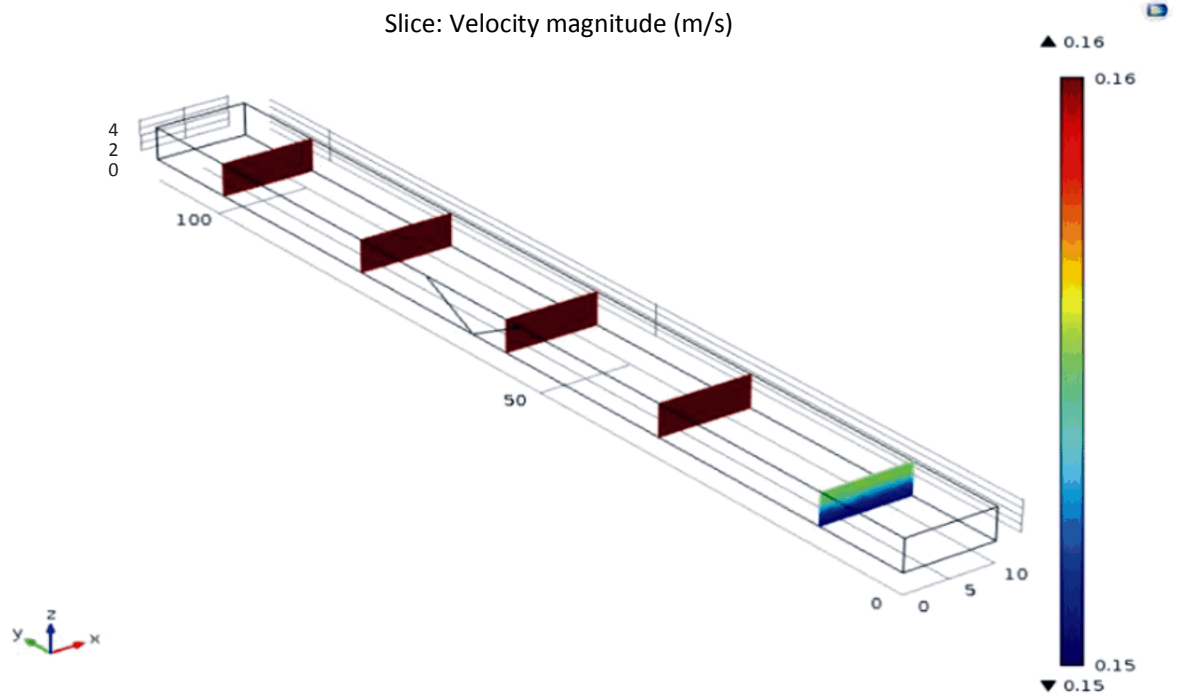


Figure 6: Velocity profile for channel with no sill height 120° V-notch side weir, having downstream weir

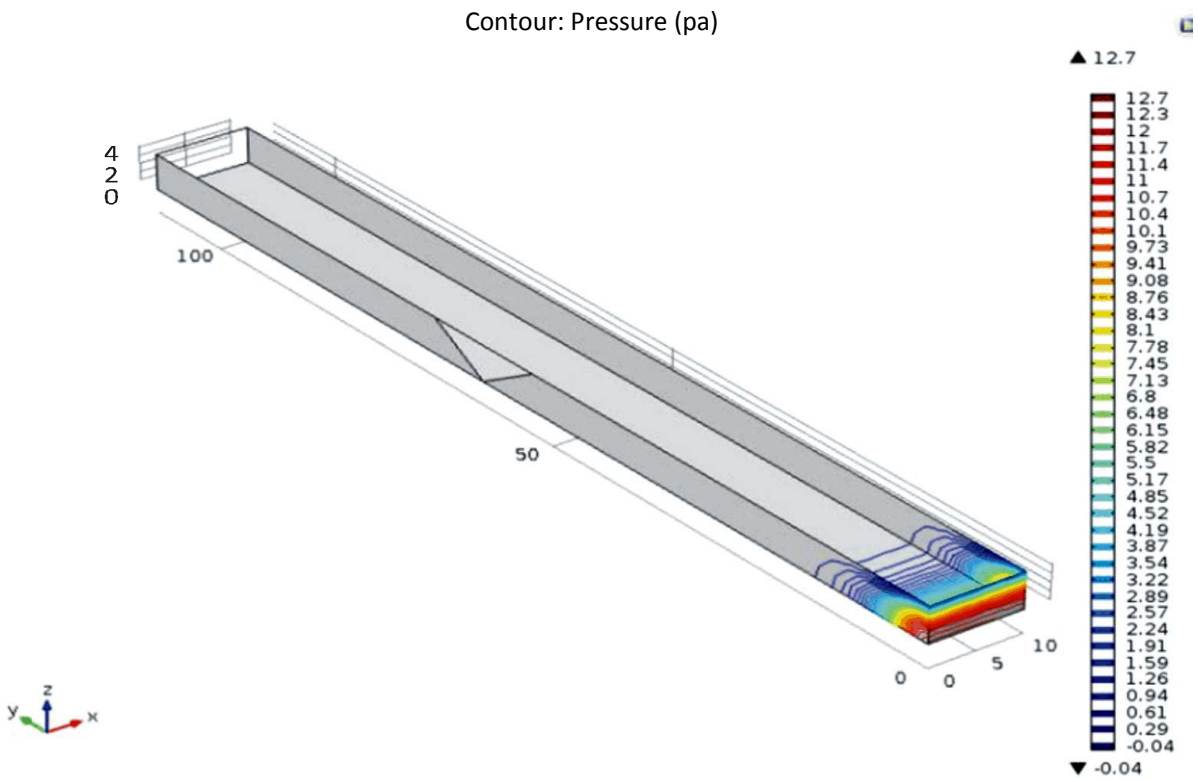


Figure 7: Pressure profile for channel with no sill height 120° V-notch side weir, having downstream weir

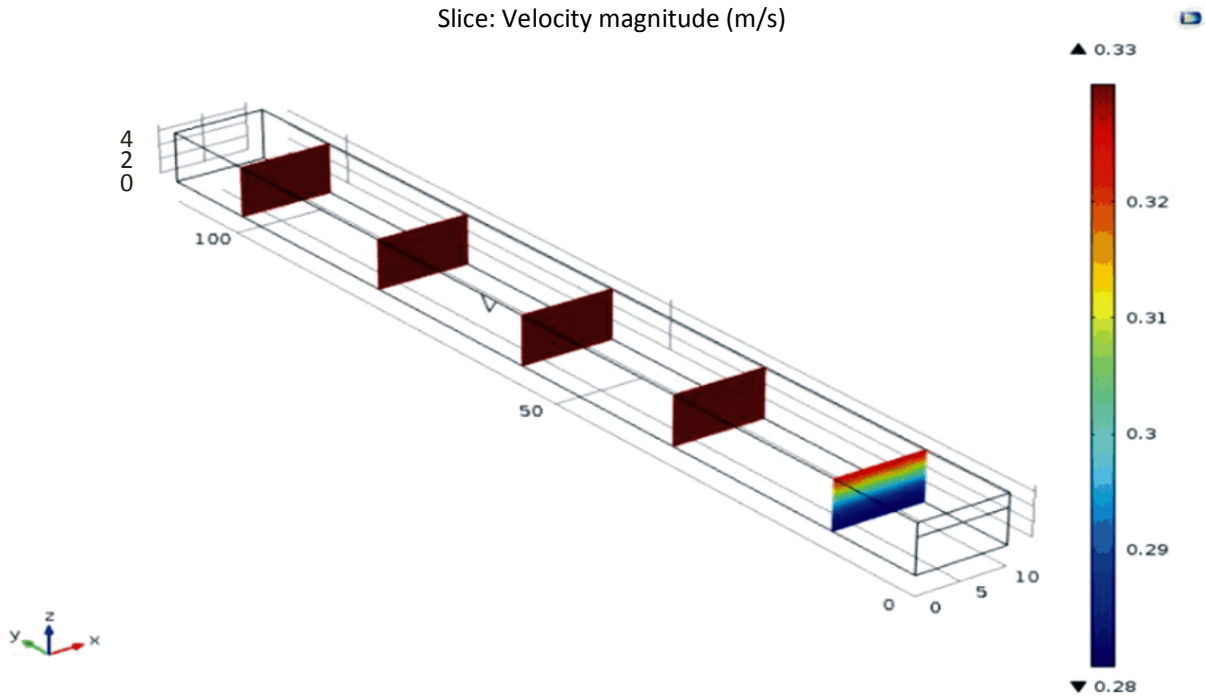


Figure 8: Velocity profile for channel with 5 cm sill height 60° V-notch side weir, having 5 cm downstream weir

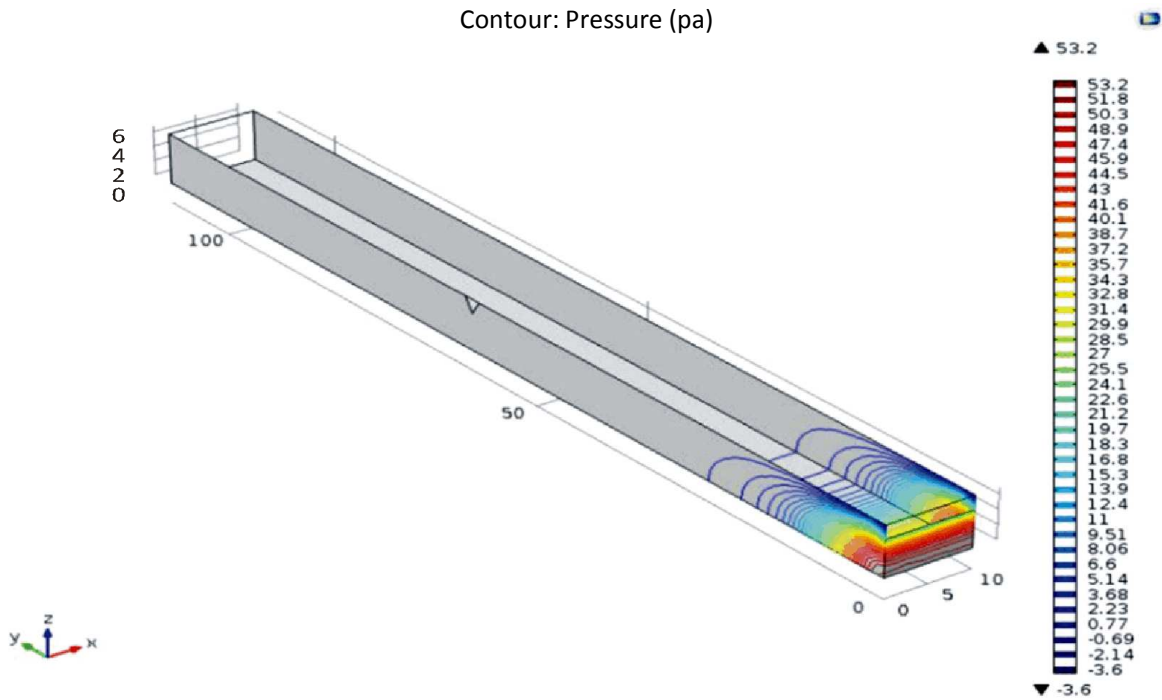


Figure 9: Pressure profile for channel with 5 cm sill height 60° V-notch side weir, having 5 cm downstream weir

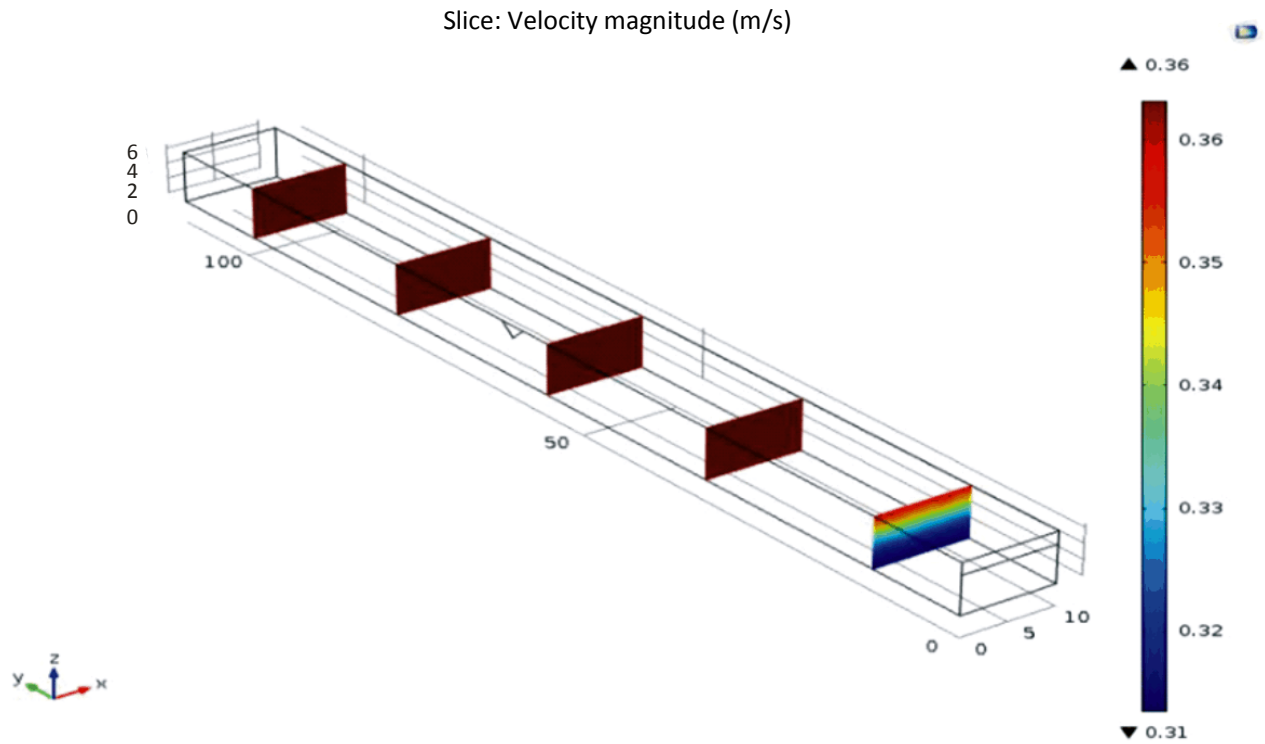


Figure 10: Velocity profile for channel with 5 cm sill height 90° V-notch side weir, having 5 cm downstream weir

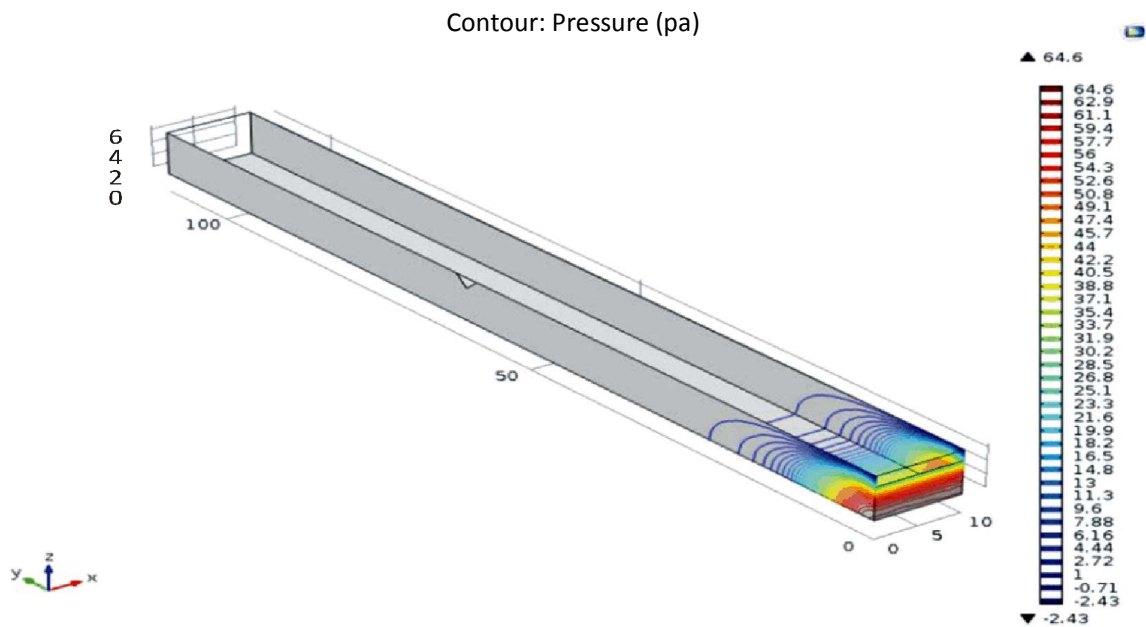


Figure 11: Pressure profile for channel with 5 cm sill height 90° V-notch side weir, having 5 cm downstream weir

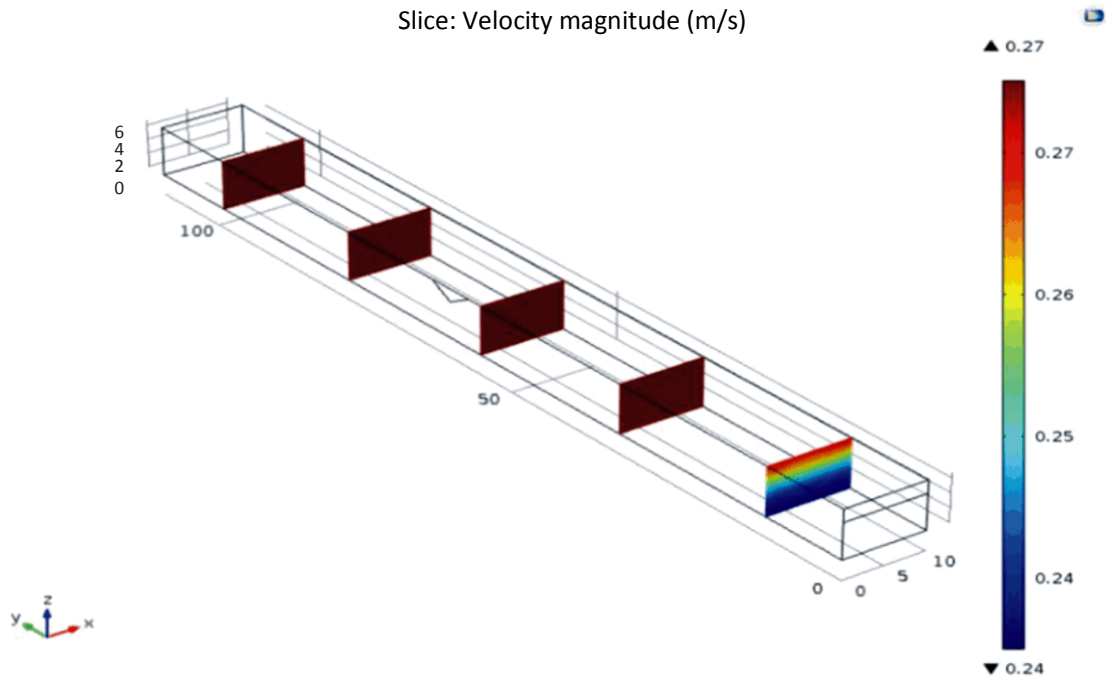


Figure 12: Velocity profile for channel with 5 cm sill height 120° V-notch side weir, having 5 cm downstream weir

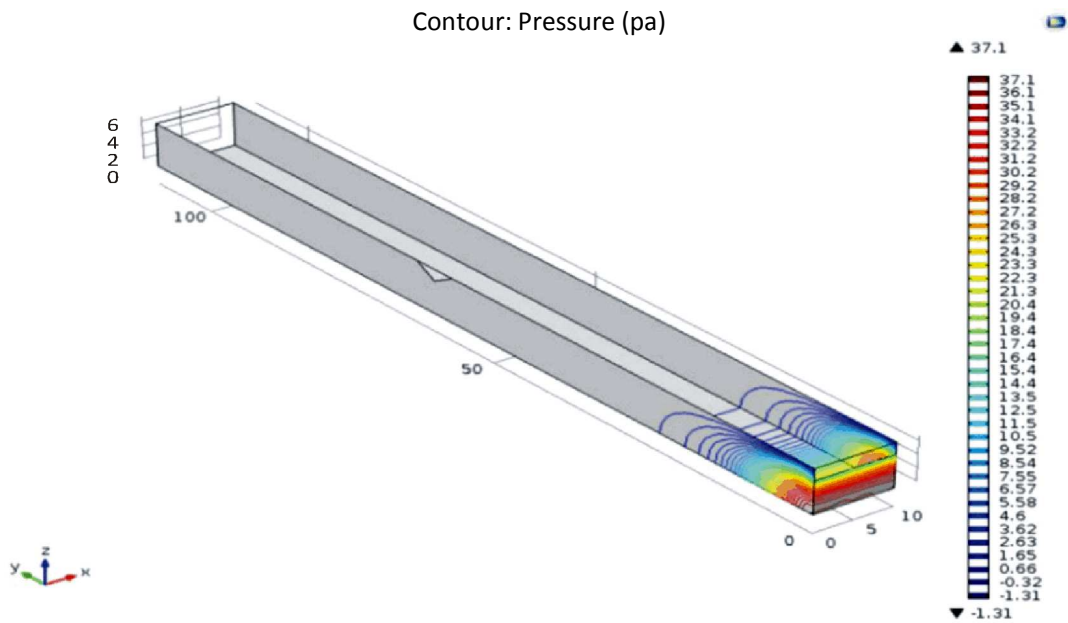


Figure 13: Pressure profile for channel with 5 cm sill height 120° V-notch side weir, having 5 cm downstream weir

**Comparison between simulation and experimental discharge coefficient**

The coefficient of discharge ( $C_d$ ) for the experiment and simulation was compared using Root Mean Square Error (RMSE) and presented in the Tables 13 and 14. The RMSE for channels with no sill height V-notch side weir, having 5 cm rectangular downstream weir tends to unity (Table 13) as the angle of V-notch increases while for channels with 5 cm sill height V-notch side weir having 5 cm rectangular

downstream, the RMSE increased as the V-notch angle increased, which implies an agreement between the experiment and the simulated discharge coefficient. For angles of 90 and 120 degrees of no sill height V-notch side weir in channels having downstream weir, the RMSE is 1 which can be inferred that the discharge coefficient for 90 and 120 degrees with no sill height V-notch side weir in a channel with downstream weir has a good agreement between the experiment and the simulation.

Table 22: Channels with no sill height V-notch side weir, having 5 cm rectangular downstream weir

| Angle | $C_d$ exp | $C_d$ sim | RMSE (%) |
|-------|-----------|-----------|----------|
| 60    | 0.93      | 0.68      | 25       |
| 90    | 0.71      | 0.71      | 1        |
| 120   | 0.73      | 0.72      | 1        |

Table 23: Channels with 5cm sill height V-notch side weir having 5 cm rectangular downstream weir

| Angle | $C_d$ exp | $C_d$ sim | RMSE (%) |
|-------|-----------|-----------|----------|
| 60    | 0.67      | 0.37      | 30       |
| 90    | 0.63      | 0.22      | 41       |
| 120   | 0.75      | 0.17      | 57       |

**Relationship between Non-Dimensional Parameters**

The results for linear regression model and the coefficient of determination (R<sup>2</sup>) for the discharge coefficient on the independent variables are presented in Tables 24-26, while the multiple regression models relationships for the discharge coefficient on the independent variables are presented in Equations (14) – (22).

Table 24: Channel with no sill height V-notch side weir having no downstream weir

| $\theta$ | $C_d f$ (Fr)        | $C_d f$ (Re)                     | $C_d f$ (H/B)                 | R <sup>2</sup> that showed variability (Fr) | R <sup>2</sup> that showed variability (Re) | R <sup>2</sup> that showed variability (H/B) |
|----------|---------------------|----------------------------------|-------------------------------|---|---|--|
| 60       | $-0.121Fr + 0.413$  | $-8.92 \times 10^{-6}Re + 0.322$ | $0.982 \frac{H}{B} + 0.148$   | 99.7%                                       |   |  |
| 90       | $0.892Fr - 0.63384$ | $-0.00012Re + 0.839$             | $-6.167 \frac{H}{B} + 1.0954$ | 92.5%                                       |   | 85.9%  |
| 120      | $-0.659Fr + 0.824$  | $-6.95 \times 10^{-5}Re + 0.424$ | $-5.3176 \frac{H}{B} + 0.755$ |   | 94%   | 100  |

**The multiple regressions models**

$$C_d = -0.175Fr - 1.547e^{-05}Re + 0.548 \quad (R^2= 1.00) \text{ for } \theta = 60 \quad (14)$$

$$C_d = 0.7769Fr - 5.505e^{-05}Re - 0.2596 \quad (R^2= 1.00) \text{ for } \theta = 90 \quad (15)$$

$$C_d = 0.4260Fr - 9.209e^{-05}Re - 0.0605 \quad (R^2= 1.00) \text{ for } \theta = 120 \quad (16)$$

From Table 24, the coefficient of determination R<sup>2</sup> of the linear regression analysis of each parameters on C<sub>d</sub> shows that 99.7% of variabilities in C<sub>d</sub> were due to Fr for 60<sup>0</sup>, 92.5% for 90<sup>0</sup>. 94% variability in C<sub>d</sub> is due to Re for 120<sup>0</sup>

while 85.9% and 100% variability in C<sub>d</sub> was due to  $\frac{H}{B}$  for 90<sup>0</sup> and 120<sup>0</sup>, respectively. However, the multiple linear regression equations 14-16 shows that only Fr and Re had 100% variability on C<sub>d</sub> for the three angles.

Table 25: Channel with no sill height V-notch side weir having 5 cm rectangular downstream weir

| $\theta$ | $C_d f$ (Fr)         | $C_d f$ (Re)                        | $C_d f$ (H/B)                   | R <sup>2</sup> that showed variability (Fr) | R <sup>2</sup> that showed variability (Re) | R <sup>2</sup> that showed variability (H/B) |
|----------|----------------------|-------------------------------------|---------------------------------|---|---|--|
| 60       | $1.4341Fr + 0.67226$ | $-8.19 \times 10^{-5}Re + 1.2889$   | $-5.1862 \frac{H}{B} + 2.9725$  |   | 91.3%                                       |  |
| 90       | $1.5567Fr + 0.28521$ | $-8.869 \times 10^{-6}Re + 0.74867$ | $-0.1995 \frac{H}{B} + 0.78463$ |   |   |  |
| 120      | $-0.995Fr + 0.436$   | $-3.67 \times 10^{-5}Re + 0.867$    | $-1.6991 \frac{H}{B} + 1.2126$  |   |   | 54%  |

**The multiple regression models**

$$C_d = 4.715e^{-05}Fr + 2.292e^{-04}Re - 0.162 \quad (R^2= 1.00) \quad \text{for } \theta = 60 \quad (17)$$

$$C_d = 5.776Fr - 0.0001Re + 0.0489 \quad (R^2= 1.00) \quad \text{for } \theta = 90 \quad (18)$$

$$C_d = 4.4968Fr - 0.0001Re - 0.0344 \quad (R^2= 1.00) \quad \text{for } \theta = 120 \quad (19)$$

From Table 25, the coefficient of determination  $R^2$  of the linear regression analysis of each parameters on  $C_d$  shows that 91.3% of variability in  $C_d$  was due to Re for  $60^\circ$  and 54% variabilities in  $C_d$  were due to  $\frac{H}{B}$  for  $120^\circ$ . However, the multiple linear regression Equations 17-19 show that only Fr and Re had 100% variability on  $C_d$  for the three angles.

Table 26: Channel with 5 cm sill height V-notch side weir having 5 cm rectangular downstream weir

| $\theta$ | $C_d f(\text{Fr})$    | $C_d f(\text{Re})$                | $C_d f(H/B)$                   | $R^2$ that showed variability (Fr) | $R^2$ that showed variability (Re) | $R^2$ that showed variability (H/B) |
|----------|-----------------------|-----------------------------------|--------------------------------|------------------------------------|------------------------------------|-------------------------------------|
| 60       | $-0.0082Fr + 0.673$   | $2.8005 \times 10^{-7}Re + 0.664$ | $0.034625 \frac{H}{B} + 0.659$ | 89.9%                              |                                    |                                     |
| 90       | $-0.429Fr + 1.2519$   | $0.00027Re + (-0.353)$            | $4.68 \frac{H}{B} + 0.206$     |                                    | 76%                                | 76.2%                               |
| 120      | $-1.644Fr + (-0.297)$ | $0.00027Re + (-0.353)$            | $-6.8372 \frac{H}{B} + 3.0634$ | 99.5%                              | 76%                                |                                     |

**The multiple regression models**

$$C_d = -0.7462Fr + 0.2280e^{-04}Re + 1.1757 \quad (R^2= 1.00) \quad \text{for } \theta = 60 \quad (20)$$

$$C_d = 1.1630Fr - 1.642e^{-05}Re + 0.3526 \quad (R^2= 1.00) \quad \text{for } \theta = 90 \quad (21)$$

$$C_d = 1.903Fr - 5.372e^{-05}Re - 0.2389 \quad (R^2= 1.00) \quad \text{for } \theta = 120 \quad (22)$$

From Table 26, the coefficient of determination  $R^2$  of the linear regression analysis of each parameters on  $C_d$  shows that 89.9% of variability in  $C_d$  is due to Fr for  $60^\circ$ , 99.5% for  $120^\circ$ . 76% variability in  $C_d$  is due to Re for  $90^\circ$  and  $120^\circ$  while 76.2% variability in  $C_d$  was due to  $\frac{H}{B}$  for  $90^\circ$ . However, the multiple linear regression equations 20-22 show that only Fr and Re had 100% variability on  $C_d$  for the three angles.

**CONCLUSIONS AND RECOMMENDATION**

The discharge coefficient of a V-notch side weir is a function of Froude number and Reynolds number with 100% coefficient of determination ( $R^2$ ) showing a strong direct and multiple linear relationships between the three variables. Channels with downstream weir as higher discharge coefficient compared with channels with no downstream weir from the analysis of the experimental results. The discharge coefficient presented can be used to accurately predict the discharge over sharp-crest V-notch side weir. A longer channel and a more sophisticated system should be considered in further studies, so as to reduce turbulence in the channel, computational time and enable finer mesh settings during simulation against the coarser mesh selected for the present study.

**REFERENCES**

Abd el-hady rady, R. M. (2011). 2D-3D Modeling of Flow Over Sharp-Crested Weirs, *J. of Applied Sciences Research* 7(12): 2495-2505.

Abdullahi, U. (2014). Experimental Investigation of Flow Characteristics Over Semi-Circular Broad Crested Weir Models. MSc. Project. Dept. of Water Resources and Environmental Engineering, Faculty of Engineering, Ahmadu Bello University, Zaria Nigeria.

Bakker, A. (2006). Applied Computational Fluid Dynamics Lecture 1 - Introduction to CFD. <http://www.bakker.org/dartmouth06/engs150/01-intro.pdf>, accessed July 2, 2017.

Douglas, J. F., Gaslorek, J. M., Swaffield, J. A. and Jack, L. B. (2005). Fluid Mechanics, Fifth Edition Pearson Education Limited Edinburgh Gate Harlow Essex CM20 2JE England. Chapter 4, 93-109.

Eghbalzadeh, A., Javan, M., Hayati, M. and Amini, A. (2015). Discharge Prediction of Circular and Rectangular Side Orifices Using Artificial Neural Networks, *KSCE J. of Civil Engineering*, 1-7.

Kuzmin D. (2016). Introduction to Computational Fluid Dynamics, <http://www.mathematik.uni-dortmund.de/~kuzmin/cfdintro/lecture1.pdf>, accessed March 10, 2017.

Mangarulkar, K. (2010). Experimental and Numerical Study of the Characteristics of Side Weir Flows, MSc. Project. Dept. of Civil and Environmental Engineering. Western University, London, Ontario, Canada.

Mohammadighavam, S. (2017). Hydrological and Hydraulic Design of Peatland Drainage and Water Treatment Systems for Optimal Control of Diffuse Pollution, Academic Dissertation of the Doctoral Training Committee of Technology and Natural Sciences. University of Oulu Graduate School; University of Oulu, Faculty of Technology.

Nezami, F., Davood, F. and Mohammad A. N. (2015). Discharge Coefficient of Trapezoidal Side Weir, *Alexandria Engineering Journal*. 54 (3): 595-605.

Ogedengbe, K. and Ewemoje, T. A. (2001). "Determination of the Discharge Coefficient of Rectangular Side Weirs, *J. of Applied Science and Technology*, 1(1), 32-37.

Parsaie, A. and Haqiabi, A. M. (2013). Development and Evaluating of Two-Neural Network Model (Mlp1 And Svm2) To Estimate the Side Weir Discharge Coefficient, *Int. J. of Agricultural Crop Science*, 5 (23), 2804-2811.

Rajput, R.K. (2013). Fluid Mechanics and Hydraulics Machines, S. Chand and Company Ltd, Ram Nagar, New Delhi, Fully Revised Multicolour Ed., Chapter 9.

Shahaboddin, S., Hossein B., Zaji A. H., Dalibor P., and Motamedi, S. (2016) Improved Side Weir Discharge Coefficient Modeling by Adaptive Neuro-Fuzzy Methodology, *KSCE Journal of Civil Engineering*, 1-7.

Spencer, P. R. (2013). Investigation of Discharge Behaviors from A Sharp-Edged Circular Orifice in Both Weir and Orifice Flow Regimes Using an Unsteady Experimental Procedure, MSc. Project. Dept. of Building, Civil and Environmental engineering. Concordia University. Montreal, Quebec, Canada.